Glycobiology, 2015, vol. 25, no. 5, 492–501
doi: 10.1093/glycob/cwu136
Advance Access Publication Date: 11 December 2014
Original Article

OXFORD

Original Article

Atomic-resolution structure of the α-galactosyl binding *Lyophyllum decastes* lectin reveals a new protein family found in both fungi and plants

André van Eerde[2,†], Elin M Grahn[2,†], Harry C Winter[3], Irwin J Goldstein[3], and Ute Krengel[1,2]

[2]Department of Chemistry, University of Oslo, PO Box 1033, Oslo NO-0315, Norway, and [3]Department of Biological Chemistry, University of Michigan, Medical School, Ann Arbor, MI 48109–0606, USA

[1]To whom correspondence should be addressed: Tel: +47 22 85 54 61; Fax: +47 22 85 54 41; e-mail: ute.krengel@kjemi.uio.no

[†]Equal contributions.

Received 23 August 2014; Revised 2 December 2014; Accepted 3 December 2014

Abstract

The crystal structure of the α-galactosyl binding *Lyophyllum decastes* lectin (LDL) was determined to 1.0 Å resolution by sulfur single-wavelength anomalous diffraction (SAD). The 10 kDa protein exhibits no sequence similarity to any protein with known structure and adopts a unique lectin fold, where a core of two antiparallel β-sheets at the heart of the homodimer is connected to the periphery of the structure by intramolecular disulfide bridges. This fold suggests that LDL is secreted, which sets it apart from other mushroom lectins. Structures of complexes between LDL and the ligands α-methylgalactoside and globotriose shed light on the binding specificity. Sequence comparison suggests a location and function of LDL and homologous proteins in or at the fungal cell wall. Structural comparison allows the identification of a superfamily of secreted proteins with the LDL fold, which may play a role at the interface between fungi and their environment.

Key words: carbohydrate recognition, fungal lectin, mushroom lectin, protein–carbohydrate interactions, X-ray crystal structure

Introduction

Lectins are proteins that specifically bind carbohydrates without catalytically modifying them. Structurally, lectins have been shown to belong to a limited number of unrelated families, with carbohydrate specificities varying substantially both between and within these families. Originally, most lectins were isolated from plant sources, but with time, lectins have been identified in all kingdoms of life. They participate in diverse biological processes where specific carbohydrate recognition is required, for example, in cell adhesion, cell–cell interactions and carbohydrate storage. Lectins also play an important role in biochemical and biomedical research, as useful diagnostic tools and markers for a specific carbohydrate (Van Damme et al. 1998). The search for lectins with novel physical properties and ligand specificities is therefore continuing. Also, the potential use of these carbohydrate-binding proteins as anti-tumor, or anti-infection agents is under investigation (Van Damme et al. 1998; Varrot et al. 2013).

Mushrooms and other fungi are comparatively less studied than other organisms and have attracted interest as a source of biomolecules with interesting novel characteristics. With respect to mushroom lectins, several structures have been published in the last few years, which show a large variability both in specificity and 3D structure, but belong mainly to previously described structural classes (Wimmerova et al. 2003; Walser et al. 2004; Birck et al. 2004; Carrizo et al. 2005; Ban et al. 2005; Mancheño et al. 2005; Cioci et al. 2006; Grahn et al. 2007; Wälti et al. 2008; Kadirvelraj et al. 2011; Angulo et al. 2011; Bovi et al. 2011; Pohleven et al. 2012; Schubert et al. 2012; Žurga et al. 2014). The biological roles of the various mushroom lectins are still unclear, even though recently a role in defense against

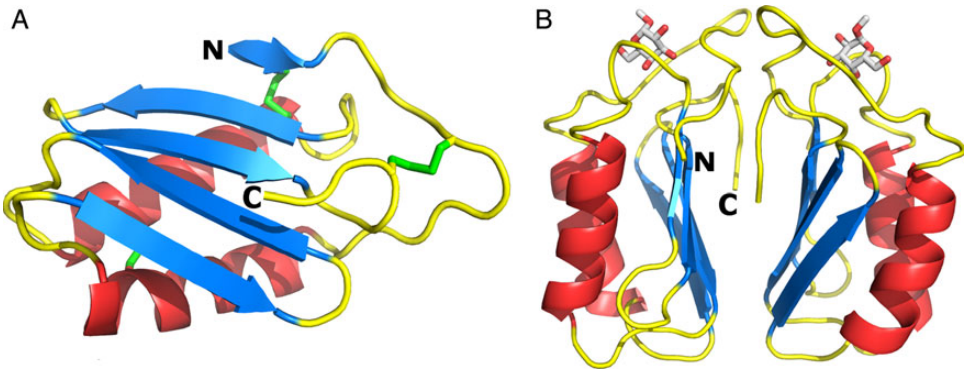

Fig. 1. Overall structure of LDL. (**A**) Structure of one LDL subunit, with disulfide bridges indicated in stick representation. (**B**) Structure of the LDL dimer showing the location of α-methylgalactoside in stick representation. N- and C-termini are indicated. This figure and Figures 2 and 4 were prepared with PyMOL (Schrödinger LLC).

predators and parasites has been proposed for a number of cytoplasmic mushroom lectins (Butschi et al. 2010; Cordara et al. 2011; Bleuler-Martínez et al. 2011; Schubert et al. 2012; Cordara et al. 2014; Žurga et al. 2014). Some of the mushroom lectins have mitogenic, anti-proliferative, anti-tumor, anti-viral and immune-stimulating activity toward mammalian cells (Yu et al. 1993; Yang et al. 2009; Cordara et al. 2014), which make them interesting for medical applications.

A few years ago, a new lectin was isolated from *Lyophyllum decastes* (Goldstein et al. 2007). This edible mushroom is used as a health-promoting supplement in Japan (Iwasa et al. 2006), and its polysaccharide extracts were shown to have anti-tumor effects (Ukawa et al. 2000). *Lyophyllum decastes* lectin (LDL) is a 10 kDa homodimeric protein recognizing non-reducing α-galactosyl groups. It has an unusual specificity for the Galα(1,4)Gal epitope, which is rare in humans (Goldstein et al. 2007). This carbohydrate constitutes the terminal part of the glycolipid globotriaosylceramide (Gb_3), the functional receptor for Shiga toxin from *Shigella dysenteriae* and Shiga-like toxins (also called verotoxins) from EHEC (entero-hemorrhagic *Escherichia coli*) (Johannes and Römer 2010), and it is also one of the targets for the pyelonephritis-associated pili protein G (PapG) adhesin from uropathogenic *E. coli* (Dodson et al. 2001). Gb_3 in pigs serves as the ligand for the streptococcal adhesin P (SadP) adhesin from *Streptococcus suis* (Kouki et al. 2011). The Galα(1,4)Gal epitope also occurs in avian (Suzuki et al. 2004) and amphibian glycoproteins (Strecker et al. 1992; Guerardel et al. 2000; Delplace et al. 2002). Interestingly, LDL shows no obvious sequence similarity to any known lectin or other protein of known function. Moreover, unlike other mushroom lectins, for which a cytosolic location can be surmised (Grahn et al. 2007; Bleuler-Martínez et al. 2011), the presence of disulfide bridges in this lectin suggests that LDL may be secreted.

Here, we report the crystal structure of this unusual lectin, which was determined with the sulfur single-wavelength anomalous diffraction (SAD) phasing method, and show that it has a novel lectin fold. The well-defined structure explains the requirement for a terminal α-galactose residue in its ligands and the specificity for α-1,4-linked galactose.

Results and discussion

Structure solution using sulfur-SAD

We attempted to solve the LDL structure by sulfur-SAD as the phasing method of choice, making use of the fact that well-diffracting crystals could easily be obtained and that the 94-residue LDL contains the relatively high number of six sulfur atoms (Goldstein et al. 2007). As no sequence homologs could be identified in the Protein Data Bank (PDB) and the protein was isolated directly from a mushroom, popular phasing methods such as molecular replacement (MR) or seleno-multi-wavelength anomalous diffraction were not feasible. Although phasing by S-SAD was already reported in 1981 (Hendrickson and Teeter 1981) and most proteins contain a fair number of sulfur atoms in their native structures, this method is currently used only to a very limited extent, with few structures solved by this method (Liu et al. 2012, 2013; Hendrickson 2013). In S-SAD, the small intensity differences caused by the anomalous dispersion of the sulfur atoms are exploited for phasing. To maximize these differences, a relatively long but accessible wavelength of 1.698 Å was used. Under these conditions, the expected Bijvoet ratio, used as an indicator for the measurability, would be 1.3%, which should be sufficient for structure determination (Ramagopal et al. 2003). A highly redundant dataset was collected to 1.68 Å on a single well-diffracting crystal of the $P2_1$ crystal form (Table I). The quality of the resulting data was sufficient to easily locate the sulfur atoms and solve the phase problem.

Overall structure

The structure of LDL was determined for two different crystal forms ($P2_1$ and $P222_1$), to high resolution of 1.00 and 1.03 Å, respectively. A complete high-quality model for LDL in the $P2_1$ crystal form could be built into the S-SAD phased map, with R/R_{free} of 0.11/0.13. The $P222_1$ structure was solved by molecular replacement using the $P2_1$ model, yielding R/R_{free} values of 0.11/0.14. The structures are essentially the same and the models all featured good geometry with low root mean square deviation (r.m.s.d.) from ideal geometry and no outliers in the Ramachandran plots (Table I).

The LDL protomer forms a compact structure, consisting of a five-stranded anti-parallel β-sheet and two α-helices packed against one side of the β-sheet (Figure 1A). The secondary structure elements are generally connected by short turns and loops. The structure is highly ordered, with the three disulfide bridges further aiding to stabilize the structure. Specifically, two cystine bridges (Cys2–Cys68 and Cys8–Cys91) tether the potentially floppy N-terminal residues tightly to the main body of the molecule, whereas the remaining disulfide bridge (Cys27–Cys57) cross-links the two α-helices (Figure 1A).

LDL is known to be dimeric from previous experiments (Goldstein et al. 2007). The dimer can be easily identified in the crystal structures and is formed by the stacking of the exposed sides of the β-sheets of the two subunits. In addition, residues 4–10, forming the first part of the loop following the short N-terminal β-strand, as well as the C-terminal

Table I. Data collection, phasing and refinement statistics

	S-SAD	$P2_1$ *apo*	$P222_1$ *apo*	α-Methylgalactoside	Globotriose
Space group	$P2_1$	$P2_1$	$P222_1$	$P2_12_12$	$P2_1$
Unit cell					
a (Å)	34.7	34.8	37.4	62.1	34.9
b (Å)	56.9	56.7	44.2	75.0	56.8
c (Å)	44.5	44.5	62.1	44.4	44.5
β (°)	107.3	107.1	90	90	107.1
Wavelength (Å)	1.698	0.934	0.931	0.931	0.934
Resolution	20–1.68 (1.73–1.68)	20–1.00 (1.06–1.00)	20–1.03 (1.09–1.03)	20–1.30 (1.38–1.30)	20–1.30 (1.38–1.30)
Completeness (%)	95.7 (64.3)	94.6 (91.7)	94.7 (86.6)	98.5 (97.2)	86.4 (46.5)
Redundancy	14.3 (5.3)	4.1 (3.9)	4.4 (2.7)	4.4 (4.4)	4.7 (2.5)
Unique reflections	35393 (1795)	84151 (13132)	50528 (7161)	50868 (7972)	35328 (3099)
$I/\sigma I$	40.4 (6.6)	14.0 (2.7)	13.9 (1.6)	15.9 (2.3)	39.7 (5.9)
R_{sym}[a] (%)	4.5 (15.2)	6.3 (50.7)	6.1 (59.0)	6.2 (64.4)	2.3 (14.9)
R_{meas}[b] (%)	4.6 (16.5)	7.3 (58.4)	7.0 (72.2)	7.0 (73.1)	2.5 (19.2)
Phasing					
S atoms	12				
F.o.m.	0.35				
Refinement					
R/R_{free}[c] (%)		10.9/12.5	11.4/13.5	17.3/21.0	12.2/15.6
No. of non-H atoms					
Protein[d]		1616	810	1558	1505
Ligand		–	–	26	34
Solvent		340	245	327	299
Avg *B* factor (Å^2)					
Protein		8.9	8.1	11	12
α-Gal				12	15
β-Gal					21
β-Glc					28
Solvent		24	24	26	28
Ramachandran (%)					
Favored		98	98	98	98
Outliers		0	0	0	0
R.m.s.d.					
Bonds (Å)		0.008	0.010	0.011	0.009
Angles (°)		1.3	1.5	1.5	1.2
PDB ID		4NDS	4NDT	4NDU	4NDV

Values in parentheses are for the highest resolution shell.
[a]$R_{sym} = \sum |I - \langle I \rangle| / \sum I$, where I is the observed intensity and $\langle I \rangle$ the average intensity.
[b]$R_{meas} = \sum_h \sqrt{\frac{n_h}{n_h - 1}} \sum_i^{n_h} |\hat{I}_h - I_{h,i}| / \sum_h \sum_i^{n_h} I_{h,i}$, where $\hat{I}_h = \frac{1}{n_h} \sum_i^{n_h} I_{h,i}$ (Diederichs and Karplus 1997).
[c]$R = \sum_{hkl,work} ||F_{obs}| - k|F_{calc}|| / \sum_{hkl} |F_{obs}|$, where F_{obs} is the observed structure factor and F_{calc} is the calculated structure factor. R_{free} is R calculated for 5% of randomly selected data that were omitted from the refinement.
[d]Including additional atoms for alternative conformations.

residues (91–94) contribute extensively to the intersubunit contacts (Figure 1B). Many hydrophobic residues are buried in the large interface area of 1001 Å^2 from a total subunit surface area of 5150 Å^2, suggesting that the LDL dimer forms a highly stable structure. The structure of LDL has no similarity to the structures of other known lectins, which establishes that LDL is the first confirmed lectin with this fold.

Ligand binding: complex of LDL with α-methylgalactoside

In order to structurally define the ligand-binding sites of this lectin, an LDL crystal was soaked in a solution containing α-methylgalactoside, which has a K_D of 1.8 mM (Goldstein et al. 2007), and diffraction data were collected (Table I). Well-defined difference electron density, characteristic of the α-methylgalactoside, was present at equivalent locations for each LDL subunit (Figure 2A and C). The ligand binds in a relatively deep, narrow and well-defined pocket on the protein surface with the two pockets separated by ~19 Å on the same face of the dimer. This arrangement of the pockets in the dimeric LDL structure may have functional relevance.

The binding pocket is shaped by the loop ranging from His69 to Asn73, the Phe13 side chain and Asn6 (Figure 2E). α-Methylgalactoside is tightly sandwiched between two amino acid residues: on one side, the hydrophobic side of the pyranose ring of galactose is stacked against the aromatic ring of Phe13, whereas on the other side, van der Waals interactions are made with Gly70. The protein engages in specific hydrogen-bonding interactions with three hydroxyl groups of the sugar residue. Specifically, OH2 forms a hydrogen bond with the carbonyl oxygen from Asn6, OH3 exhibits a hydrogen bond with the Asn73 side chain, and OH4 forms one hydrogen bond with the amide NH group of Gly70 and another with the carbonyl oxygen atom of Ser72 (Figure 2E, Table II). When comparing the α-methylgalactoside complex with the apo structure, no structural

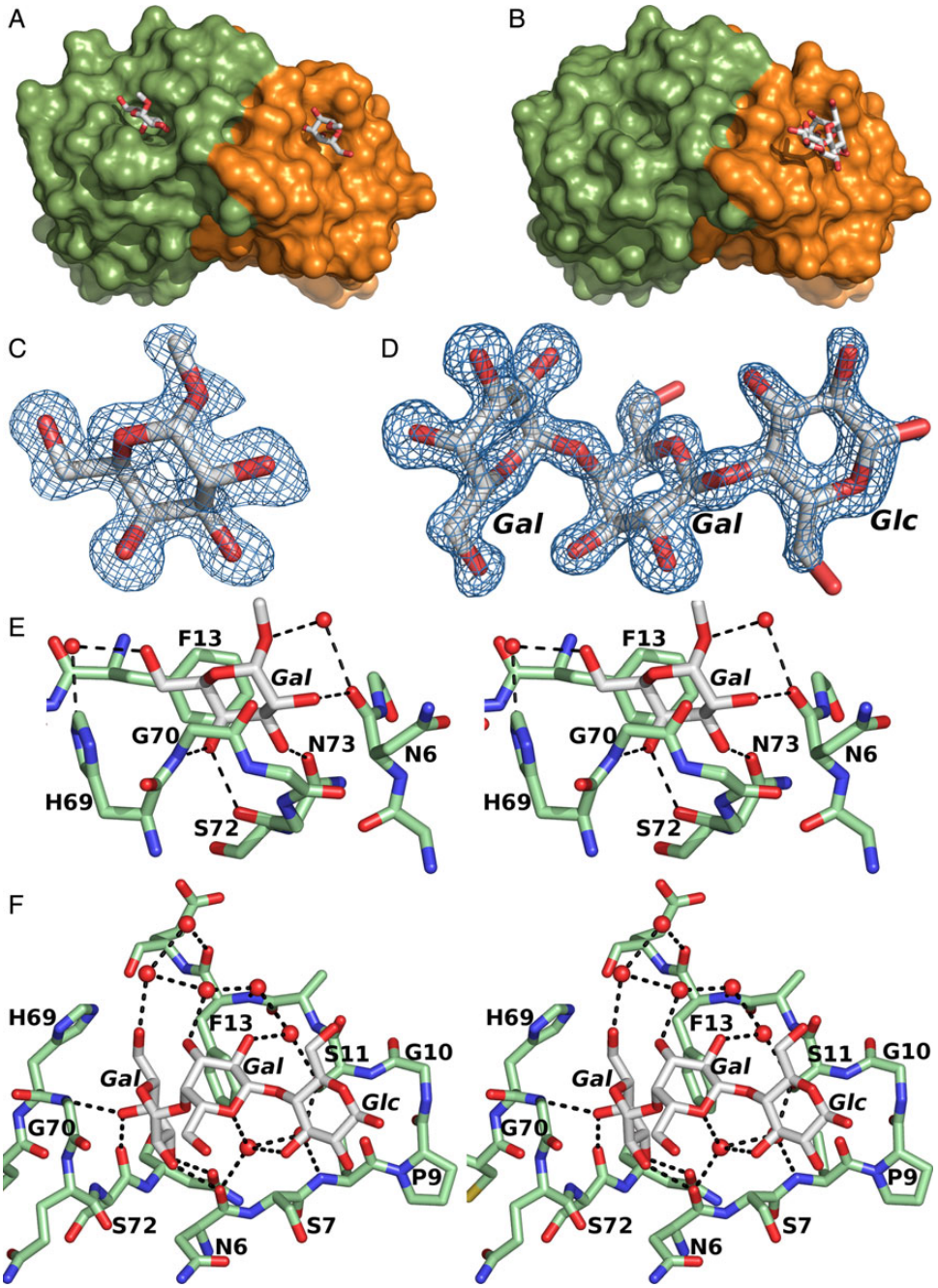

Fig. 2. Carbohydrate binding to LDL. Surface representations of LDL in complexes with (**A**) α-methylgalactoside or (**B**) globotriose (in stick representations). Simulated annealing $F_O - F_C$ OMIT density contoured at 3σ (blue mesh) of (**C**) α-methylgalactoside and (**D**) globotriose. Stereo view of interactions between LDL and (**E**) α-methylgalactoside or (**F**) globotriose. Hydrogen bonds are indicated with dashed lines. Relevant water molecules are shown as red spheres.

changes are observed in the binding pocket, illustrating the rigidity of the pocket.

Ligand binding: globotriose

In order to structurally characterize LDL's specificity for larger carbohydrate ligands, an LDL crystal was soaked with globotriose (Gal-α1,4-Gal-β1,4-Glc). This compound serves as a representative example of a 1,4-linked glycan, for which LDL has a stronger affinity (K_D of 0.38 mM compared with 1.8 mM for the monosaccharide) (Goldstein et al. 2007). Well-defined electron density was present at one of the binding sites identified in the LDL-α-methylgalactoside complex structure (Figure 2B and D). The terminal α-galactose residue binds in the exact same fashion to the pocket as seen in that structure, and the two additional carbohydrate residues extend from the α-galactose-binding pocket parallel to the relatively flat part of the LDL surface largely made up by loop 1 (residues 4–15) (Figure 2F). Interestingly, this loop is held rigidly in its conformation by the disulfide bridge Cys8–Cys91. No binding is observed in the second α-galactose-binding pocket of the LDL dimer. This may be attributed

Table II. Protein–carbohydrate interactions

	α-Methylgalactoside complex			Globotriose complex		
Residue	ASA (Å^2)	H-bonding distance [Å]	Donor–acceptor	ASA (Å^2)	H-bonding distance [Å]	Donor–acceptor
Asn6	22/24	2.8/2.7	O-O2 αGal	25	2.7	O-O2 αGal O-O5 βGal via water O-O3 βGlc via water
Ser7				19		
Cys8				4		
Ser11				23		OG-O2 βGal via water
Phe13	37/35			47		
His69	18/18		NE2-O6 αGal via water	20		NE2-O6 αGal via water
Gly70	34/32	2.9/3.0	N-O4 αGal	33	3.0	N-O4 αGal
Gln71	4/4			4		
Ser72	8/8	2.7/2.7	O-O4 αGal	9	2.4/3.0[a]	O-O4 αGal
Asn73	1/1	2.9/2.9	OD1-O3 αGal	1	2.8	OD1-O3 αGal
Phe88	1/1			1		
Total	124/121			185		

Distances and donor–acceptor pairs are listed for hydrogen bonds (as judged from distances of max. 3.2 Å and favorable angles). Accessible surface areas (ASAs) of the protein, buried by the ligand, are listed. The two values given for interactions in the α-methylgalactoside complex are from the two crystallographically independent copies in the model.

[a]Distances for two alternative conformations of Ser72.

to the restricted space around this pocket in the crystal lattice, as residues from loop 1 in this subunit are involved in crystal contacts. The β-galactose and β-glucose residues have higher temperature factors than the α-galactose residue, which is indicative of a higher disorder, consistent with the absence of direct contacts between the protein and these sugar residues (Table II). Only a few water-mediated interactions between LDL and the second β-galactose residue are observed, and the terminal β-glucose residue is even farther away from the LDL surface and has even weaker water-mediated interactions (Figure 2F). The limited interactions found in this complex for the β-galactose and β-glucose residues are consistent with the modest increase in affinity for globotriose compared with α-galactose alone.

Specificity of ligand binding

Taken together, these structures allow some pertinent insights into the previously reported binding specificity of this lectin (Goldstein et al. 2007). The shape of the narrow binding pocket is highly complementary to the dimensions of α-galactose. Specifically, epimers at the C2, C3 and C4 positions would not be able to occupy this pocket without clashes. A comparison of the activity studies with the current structural data suggests that LDL has an absolute requirement for an axial hydroxyl at the C4 position, explaining its selectivity for galactose. In fact, the only other somewhat acceptable monosaccharide ligand is methyl-β-D-fructopyranoside (Goldstein et al. 2007), which shares the axial hydroxyl group at the C4 position, but would otherwise not completely fill the binding site. Also the β-anomer of galactose would experience steric hindrance, with Gly70. Taken together, the structure and rigidity of this pocket determines the marked preference for α-galactose, and gives LDL a much narrower specificity for α-galactose than several other α-galactosyl-binding lectins. These lectins, such as the rhamnose-binding chum salmon lectin 3 (Shirai et al. 2009), the legume lectin basic winged-bean agglutinin (Kulkarni et al. 2008) and lectins from the jacalin family (Sankaranarayanan et al. 1996; Rao et al. 2004; Sharma et al. 2009), generally use wider pockets or grooves, which make less extensive and less complementary interactions with α-galactose. On the other hand, the extensive interactions in a narrow and deep pocket on the lectin surface are reminiscent of the manner in which the legume lectin *Griffonia simplifica* lectin I B_4 (GS I-B_4) from *Griffonia simplifica* achieves a high specificity for α-galactose (Tempel et al. 2002).

Unlike GS I-B_4, LDL shows enhanced specificity for certain di- and trisaccharides, with globotriose (Gal-α1,4-Gal-β1,4-Glc) being the best currently known ligand of LDL (Goldstein et al. 2007). Our structural data can attribute this to the modest contributions to the lectin–ligand interactions made by the two additional sugar residues, winding along the surface of LDL. As all interactions with the second carbohydrate residue are water-mediated, it can be expected that LDL can accommodate not only galactose but also other sugar residues in this position. The curvature of the globotriose ligand in its minimum-energy conformation (Cummings et al. 1998) complements the convex shape of the LDL surface in this area. Manual modeling suggests that no steric constraints would preclude binding of Gal-α1,2- and Gal-α1,3-linked terminal disaccharide moieties, but terminal disaccharides would likely have varying degrees of interaction with LDL, allowing LDL to exhibit some specificity. LDL binding of oligosaccharides clearly differs from GS I-B_4 in this respect. In GS I-B_4, only the terminal α-galactose contributes to binding and any other residues extend away from the protein surface (Tempel et al. 2002), which makes this lectin relatively nonspecific for the type of linkage.

LDL shares its globotriose specificity with the Shiga-like toxin I B subunit (SltIB, also known as verotoxin), which binds to the globotriose moiety of the Gb_3 glycolipid (Ling et al. 1998). Interestingly, LDL was found to not bind Gb_3, even though it has specificity for globotriose (Goldstein et al. 2007). The SltIB pentamer is able to bind 15 Gb_3 molecules, which amounts to three structurally different binding sites per subunit (Ling et al. 1998). The globotriose moieties all adopt a similar conformation when bound to the toxin, but the actual binding sites, which in SltIB resemble shallow concave grooves, are different in character when compared with the LDL-globotriose complex. In addition, SltIB only interacts with the "convex" side of the trisaccharide (Ling et al. 1998), while LDL binds to the "concave" side of the trisaccharide. The binding of globotetraose (GalNAc-β1,3-Gal-α1,4-Gal-β1,4-Glc) to the PapG fimbrial adhesion of uropathogenic *E. coli* resembles the globotriose binding to SltIB in this respect (Dodson et al. 2001), and also *Pseudomonas aeruginosa* lectin

probably binds the globotriose moiety of Gb_3 in a similar manner compared with SltIB (Blanchard et al. 2008). It is possible that this difference in binding mode precludes Gb_3 from binding to LDL, analogous to what has been proposed to explain the greater efficiency of binding of Gb_3 over isoglobotriaosylceramide to *P. aeruginosa* lectin, even though the lectin has the same affinity for the trisaccharide moieties (Blanchard et al. 2008). The conformation of Gb_3 in a membrane environment reportedly shields the side of the globotriose moiety that interacts most extensively with LDL (Fantini 2007). This makes it unlikely that membrane-embedded Gb_3 is the natural ligand for LDL, and furthermore suggests that LDL can be used as a specific probe for α1,4-linked terminal galactose units of non-glycolipid nature.

LDL may identify a protein family common to fungi

LDL is present in significant amounts in the fruiting bodies of *L. decastes*, but its natural interaction partner and its role there are unknown. Even though it is known that *L. decastes* produces galactose-containing polysaccharides (Ukawa et al. 2000), no data are available regarding their linkage type. To shed more light on the possible function of LDL in *L. decastes*, an attempt to identify potential homologs of LDL was made. Interestingly, only sequences derived from fungi gave significant hits in a BLAST search for homologous proteins among the non-redundant sequences in Genbank. The highest homology was found with a putative protein from the mushroom *Trametes versicolor*, with 27% sequence identity. PSI-BLAST runs iterated until convergence identified with high confidence several more distantly related sequences up to a total of ~25 which share <80% sequence identity among each other (Figure 3). Interestingly, all those sequences derived from fungi, but not all sequenced fungal genomes contain readily identifiable LDL homologs. An alignment of the sequences of LDL homologs suggests a broad conservation of secondary structure elements, as well as the general conservation of two of the three disulfide bridges found in LDL (Figure 3). The residues, which define specific LDL characteristics, such as those involved in dimer formation are, however, only conserved in the closest LDL homologs in mushrooms (Figure 3). The residues, which in LDL shape the α-galactosyl-binding pocket and the surrounding area, are not highly

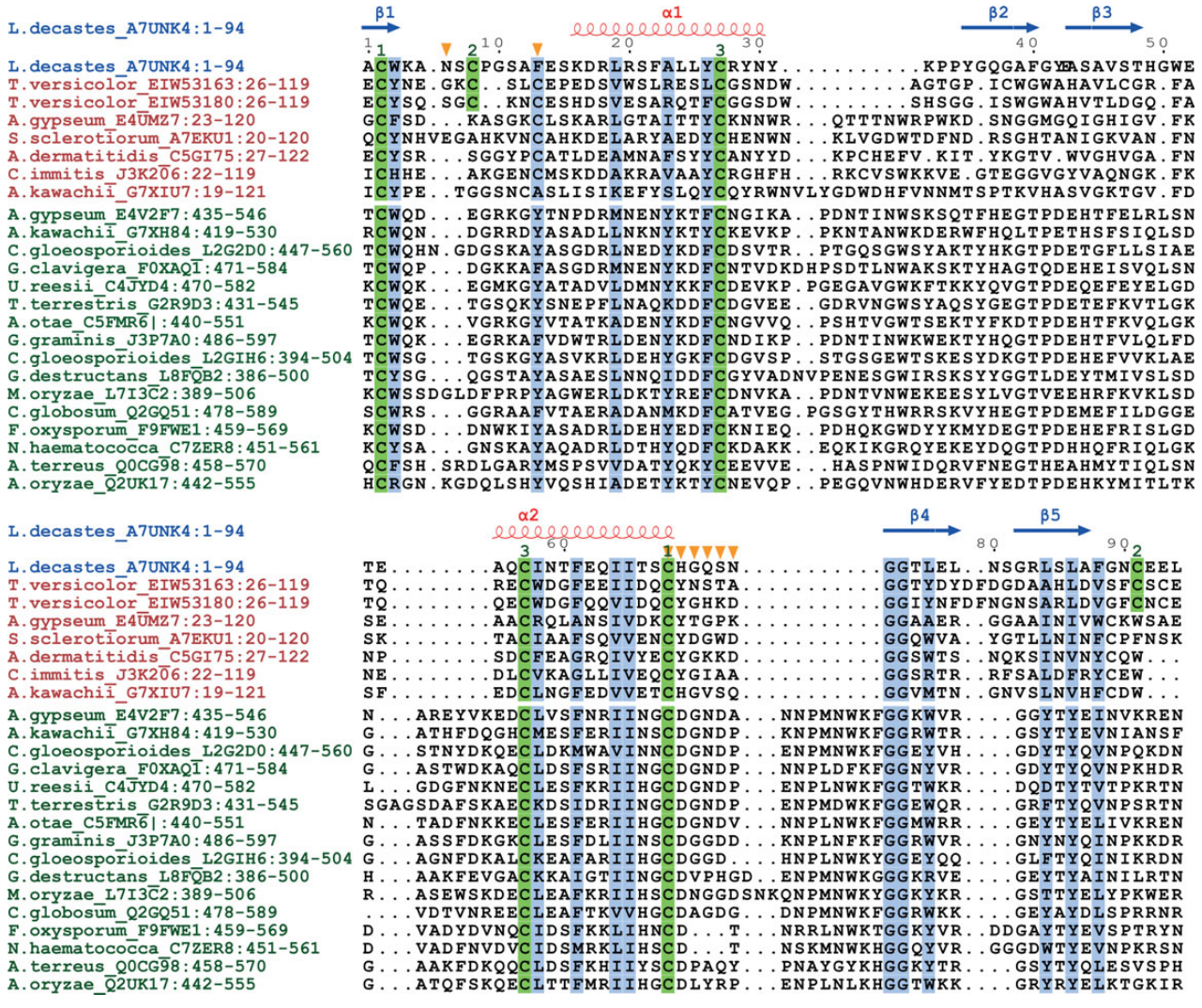

Fig. 3. Sequence alignment of LDL with fungal homologs. Secondary structural elements of LDL are indicated above the sequence. Conserved residues are highlighted. LDL residues forming the α-galactose binding pocket are indicated with orange triangles above the sequence, LDL disulfide bridges are labeled with numbers above the sequence, with the names of single-domain LDL homologues in red, and names of homologs fused to SGNH-family proteins in green. Most sequences are labeled with their species origin and Uniprot code, except for the *T. versicolor* draft sequences, which are labeled with their Genbank codes.

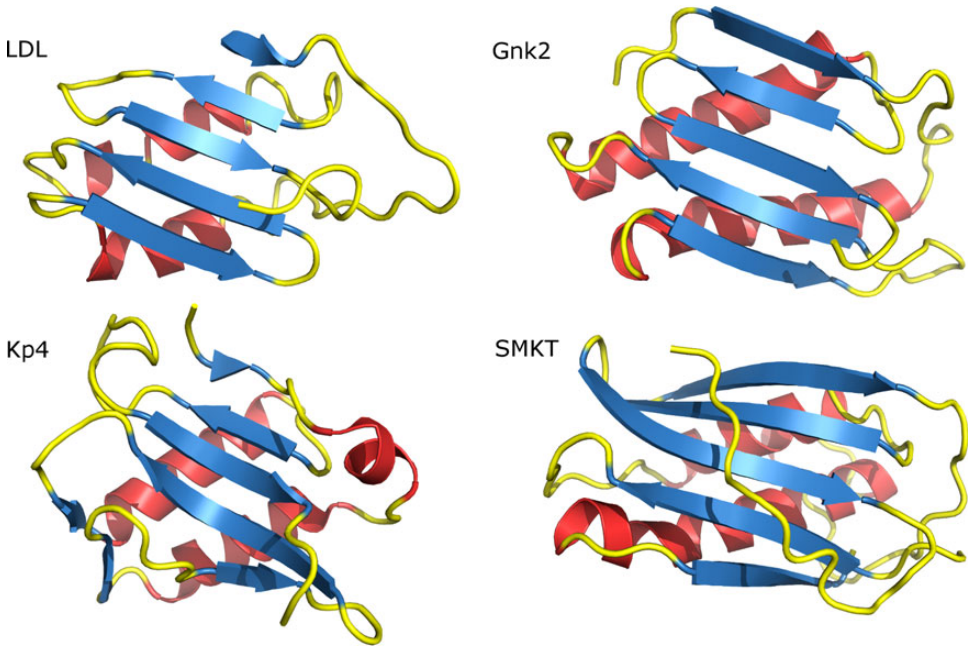

Fig. 4. LDL, ginkbilobin-2, killer protein 4 and SMKT share the same fold. Structures of LDL, *Ginkgo biloba* Ginkbilobin-2 (PDB ID: 3A2E; Miyakawa et al. 2009), *Ustilago maydis* KP4 (PDB ID: 1KPT; Gu et al. 1995) and *Pichia farinosa* (PDB ID: 1KVE; Kashiwagi et al. 1997), are shown in the same orientation.

conserved either. The presence of an N-terminal signal peptide (at least in all LDL homologs) and conserved cysteines, which in LDL are involved in disulfide bridges, suggest that all of the encoded proteins are secreted. Taken together, this suggests that even though sequence homologs of LDL exist in other fungi, their precise activities and functions may not be conserved.

Further analysis shows that the homologous sequences can be divided into two groups, where the proteins in the group with closest homology to LDL only consist of a single LDL-like domain (Figure 3). In the second group of sequences, the LDL-like domain is found at the C-terminal end of a larger domain with homology to members of the Ser, Gly, Asn, His consensus sequence (SGNH)-hydrolase family (Mølgaard et al. 2000), which is part of the Gly, Asp, Ser, Leu motif-esterase/lipase superfamily (Akoh et al. 2004). SGNH hydrolases form a family of esterases, which have a very diverse set of activities and substrates and include acetylxylan esterases, arylesterases and acetylesterases, with some of them known to modify cell-wall components. Members of this family have been found fused to other domains known to be involved in cell-surface adhesion (Anantharaman and Aravind 2010). LDL-like domains in multidomain proteins could therefore have a similar function in facilitating adhesion of an enzyme to the fungal cell wall. Interestingly, LDL shows no sequence or structural similarity to known carbohydrate-binding modules (CBMs) (Lombard et al. 2014). Our results might therefore point toward a previously unidentified class of CBMs.

LDL-like proteins may form part of a superfamily of fungal and plant proteins

No sequence similarity could be detected between LDL and proteins of known structure. However, comparison of the LDL structure with known structures deposited in the PDB (www.wwpdb.org) by 3D alignment shows that three proteins nevertheless have significant structural similarity to LDL (Figure 4). The protein with the highest similarity is ginkbilobin-2, a protein with apparent anti-fungal properties isolated from the seeds of the ginkgo biloba tree (Miyakawa et al. 2009). LDL and ginkbilobin-2 have the same fold with an r.m.s. difference for Cα atoms of 2.6 Å over 78 aligned residues, even though there is no significant sequence identity. The greatest structural divergences are found in the area that forms the carbohydrate-binding site in LDL. Ginkbilobin-2 is the only member of the domain of unknown function 26 (DUF26) protein family (PFAM: PF01657) (Chen 2001), for which the structure has been determined. DUF26 domains are found in plant proteins, to which in general a function in response to stress or fungal or bacterial pathogens is ascribed (Chen 2001; Engelmann et al. 2008).

Interestingly, the other structurally similar proteins also have antifungal properties. The virally encoded fungal toxin killer protein 4 (KP4) from the filamentous maize smut fungus *Ustilago maydis* (Gu et al. 1995) has an r.m.s.d. of 2.9 Å over 77 structurally aligned residues with LDL. KP4 is able to kill sensitive *Ustilago* strains by blocking L-type voltage-gated calcium channels (Gage et al. 2002), even though it remains unclear whether the blocking involves a direct interaction between the toxin and the calcium channel. Genes encoding putative homologs of KP4 can be detected in several other fungi and one moss (Brown 2011). The heterodimer formed by the salt-mediated killer toxin from the halotolerant yeast *Pichia farinosa* (Kashiwagi et al. 1997) has an r.m.s.d. of 3.6 Å over 79 aligned residues of LDL. This toxin can kill several genera of yeasts. Its action involves a reversible interaction with an as yet unidentified component of the yeast cell membrane (Suzuki et al. 2001). The available data on these proteins do not rule out that carbohydrate-binding properties have a role in their function.

Solving the structure of LDL and observing the structural similarity among these four proteins, which was not previously anticipated, now allows us to define a novel structural superfamily of extracellular proteins and protein domains, many of which function at an interspecies interface involving fungi and/or plants. The structural relation between these various proteins is striking. At present, the possibility that

they evolved from a common ancestor retaining similar functions cannot be ruled out, however, further data are necessary to resolve this issue. Therefore, whether LDL also has a role in interspecies warfare or has a more innocuous role, remains to be investigated.

Materials and methods

Crystallization

LDL was isolated from fruiting bodies of the mushroom *Lyophyllum decastes* and affinity-purified on a melibiose-Sepharose column as described previously (Goldstein et al. 2007). The purified protein was lyophilized and dissolved in 10 mM Tris–HCl (pH 7.5) to a concentration of 10 mg mL^{-1}. The hanging-drop vapor-diffusion technique was used to test crystallization conditions with initial drop sizes 1 + 1 µL and 0.5 mL in the wells. Crystals were obtained in several conditions using Structure Screen 1 from Molecular Dimensions (Molecular Dimensions Ltd., UK) at room temperature (293 K). The crystals showing the best X-ray diffraction properties were grown in 0.2 M $CaCl_2$, 0.1 M NaHEPES (pH 7.5) and 28% (v/v) PEG400 (space group $P2_1$), or in 0.2 M Li_2SO_4, 0.1 M Tris–HCl (pH 8.5) and 30% (w/v) PEG4000 (space group $P222_1$ or $P2_12_12$). The carbohydrates methyl α-D-galactoside (Sigma-Aldrich) and globotriose (Dextra Laboratories, UK) were dissolved in 10 mM Tris–HCl (pH 7.0) to a concentration of 10 mM, and 1 µL of the respective solutions was added directly to drops containing crystals for ~30 min. Prior to data collection, the apo-form and carbohydrate-soaked crystals were flash-frozen in liquid nitrogen without any additional cryo-protectants.

Data collection and processing

All data were collected at 100 K. The $P222_1$ and $P2_12_12$ datasets were collected at beamline ID14-3, ESRF, Grenoble, France using an ADSC Q4R CCD detector, while data for the $P2_1$ crystal form, with or without globotriose, were collected at ESRF beamline ID14-1 using an ADSC Q210 CCD detector. Data were integrated and scaled with XDS (Kabsch 2010) and programs from the CCP4 package (Winn et al. 2011). Data collection statistics are summarized in Table I.

S-SAD phasing

For a $P2_1$ LDL crystal, in addition a high-multiplicity dataset was collected to 1.68 Å resolution at ESRF beamline BM14 at a wavelength of 1.698 Å, using a Mar225 CCD detector. The data were integrated and scaled with XDS (Kabsch 2010) and programs from the CCP4 package (Winn et al. 2011). Disulfide sites were identified from data truncated to 2.2 Å using ShelXD (Sheldrick 2008) as "super-Sulfurs". Phasing was performed on the full dataset in PHASER (McCoy et al. 2007). Density modification was done with RESOLVE (Terwilliger 2000).

Model building, refinement and analysis

The model of LDL was built by cycles of manual building with Coot (Emsley et al. 2010) and refinement against the $P2_1$ dataset with Refmac5 (Murshudov et al. 2011). Final refinement was done with phenix.refine (Adams et al. 2010) and included full anisotropic *B* factor refinement. The structure of LDL in other crystal forms was solved by MR using MOLREP (Vagin and Teplyakov 2010) using one subunit as a search model. The refinement of the high-resolution model of the $P222_1$ crystal form was then done in a similar fashion as described for the $P2_1$ *apo* model. For the LDL:ligand complexes, ligands were added in places where there was sufficient difference density. The LDL:α-methylgalactoside and LDL:globotriose models only included anisotropic *B* factor refinement for all protein atoms. A riding hydrogen model was used throughout refinement for all models, with the exception of the $P2_1$ *apo* and $P222_1$ *apo* models, where individual refinement of all hydrogen atoms was performed in the final rounds of refinement. PISA (Krissinel and Henrick 2007) was used for surface area calculations, PDBeFold (Krissinel and Henrick 2004) for structure comparison, and AREAIMOL (Tickle 2007) for calculating accessible surface areas.

Acknowledgements

We thank the ESRF for beam time, Mats Ökvist, Åsmund K. Røhr, Gelareh Askarieh and Rosmarie Friemann as well as the staff of the EMBO'07 course on Exploiting Anomalous Scattering in Macromolecular Structure Determination (Grenoble 2007) for help with data collection.

Conflict of interest statement

None declared.

Funding

This work was supported by grants from EMBIO (position of E.M.G.), the Norwegian Research Council (grants no. 171631/V40 and 183613/S10 (FUGE-GlycoNor)) as well as by the University of Oslo.

Abbreviations

ASA, accessible surface area; CBM, carbohydrate-binding module; DUF, domain of unknown function; Gb_3, globotriaosylceramide; GS I-B_4, *Griffonia simplifica* lectin I B_4; KP4, killer protein 4; LDL, *Lyophyllum decastes* lectin; MR, molecular replacement; PapG, pyelonephritis-associated pili protein G; PDB, Protein Data Bank; r.m.s.d., root mean square deviation/difference; SAD, single-wavelength anomalous diffraction; SltIB, Shiga-like toxin I B subunit.

References

Adams PD, Afonine PV, Bunkoczi G, Chen VB, Davis IW, Echols N, Headd JJ, Hung LW, Kapral GJ, Grosse-Kunstleve RW, et al. 2010. PHENIX: A comprehensive Python-based system for macromolecular structure solution. *Acta Crystallogr D Biol Crystallogr*. 66:213–221.

Akoh CC, Lee GC, Liaw YC, Huang TH, Shaw JF. 2004. GDSL family of serine esterases/lipases. *Prog Lipid Res*. 43:534–552.

Anantharaman V, Aravind L. 2010. Novel eukaryotic enzymes modifying cell-surface biopolymers. *Biol Direct*. 5:1.

Angulo I, Acebrón I, de las Rivas B, Muñoz R, Rodríguez-Crespo I, Menéndez M, García P, Tateno H, Goldstein IJ, Pérez-Agote B, et al. 2011. High-resolution structural insights on the sugar-recognition and fusion tag properties of a versatile β-trefoil lectin domain from the mushroom *Laetiporus sulphureus*. *Glycobiology*. 21:1349–1361.

Ban M, Yoon HJ, Demirkan E, Utsumi S, Mikami B, Yagi F. 2005. Structural basis of a fungal galectin from *Agrocybe cylindracea* for recognizing sialoconjugate. *J Mol Biol*. 351:695–706.

Birck C, Damian L, Marty-Detraves C, Lougarre A, Schulze-Briese C, Koehl P, Fournier D, Paquereau L, Samama J-P. 2004. A new lectin family with structure similarity to actinoporins revealed by the crystal structure of *Xerocomus chrysenteron* lectin XCL. *J Mol Biol*. 344:1409–1420.

Blanchard B, Nurisso A, Hollville E, Tétaud C, Wiels J, Pokorná M, Wimmerová M, Varrot A, Imberty A. 2008. Structural basis of the preferential binding for globo-series glycosphingolipids displayed by *Pseudomonas aeruginosa* lectin I. *J Mol Biol*. 383:837–853.

Bleuler-Martínez S, Butschi A, Garbani M, Wälti MA, Wohlschlager T, Potthoff E, Sabotič J, Pohleven J, Lüthy P, Hengartner MO, et al. 2011. A lectin-mediated resistance of higher fungi against predators and parasites. *Mol Ecol*. 20:3056–3070.

Bovi M, Carrizo ME, Capaldi S, Perduca M, Chiarelli LR, Galliano M, Monaco HL. 2011. Structure of a lectin with antitumoral properties in king bolete (*Boletus edulis*) mushrooms. *Glycobiology*. 21:1000–1009.

Brown DW. 2011. The KP4 killer protein gene family. *Curr Genet*. 57:51–62.

Butschi A, Titz A, Wälti MA, Olieric V, Paschinger K, Nöbauer K, Guo X, Seeberger PH, Wilson IBH, Aebi M , et al. 2010. *Caenorhabditis elegans* N-glycan core β-galactoside confers sensitivity towards nematotoxic fungal galectin CGL2. *PLoS Pathog*. 6:e1000717.

Carrizo ME, Capaldi S, Perduca M, Irazoqui FJ, Nores GA, Monaco HL. 2005. The antineoplastic lectin of the common edible mushroom (*Agaricus bisporus*) has two binding sites, each specific for a different configuration at a single epimeric hydroxyl. *J Biol Chem*. 280:10614–10623.

Chen Z. 2001. A superfamily of proteins with novel cysteine-rich repeats. *Plant Physiol*. 126:473–476.

Cioci G, Mitchell EP, Chazalet V, Debray H, Oscarson S, Lahmann M, Gautier C, Breton C, Perez S, Imberty A. 2006. β-propeller crystal structure of *Psathyrella velutina* lectin: an integrin-like fungal protein interacting with monosaccharides and calcium. *J Mol Biol*. 357:1575–1591.

Cordara G, Egge-Jacobsen W, Johansen HT, Winter HC, Goldstein IJ, Sandvig K, Krengel U. 2011. *Marasmius oreades* agglutinin (MOA) is a chimerolectin with proteolytic activity. *Biochem Biophys Res Commun*. 408:405–410.

Cordara G, Winter HC, Goldstein IJ, Krengel U, Sandvig K. 2014. The fungal chimerolectin MOA inhibits protein and DNA synthesis in NIH/3T3 cells and may induce BAX-mediated apoptosis. *Biochem Biophys Res Commun*. 447:586–589.

Cummings MD, Ling H, Armstrong GD, Brunton JL, Read RJ. 1998. Modeling the carbohydrate-binding specificity of pig edema toxin. *Biochemistry*. 37:1789–1799.

Delplace F, Maes E, Lemoine J, Strecker G. 2002. Species specificity of O-linked carbohydrate chains of the oviducal mucins in amphibians: structural analysis of neutral oligosaccharide alditols released by reductive β-elimination from the egg-jelly coats of *Rana clamitans*. *Biochem J*. 363:457–471.

Diederichs K, Karplus PA. 1997. Improved *R*-factors for diffraction data analysis in macromolecular crystallography. *Nat Struct Biol*. 4:269–275.

Dodson KW, Pinkner JS, Rose T, Magnusson G, Hultgren SJ, Waksman G. 2001. Structural basis of the interaction of the pyelonephritic *E. coli* adhesin to its human kidney receptor. *Cell*. 105:733–743.

Emsley P, Lohkamp B, Scott WG, Cowtan K. 2010. Features and development of Coot. *Acta Crystallogr D Biol Crystallogr*. 66:486–501.

Engelmann JC, Schwarz R, Blenk S, Friedrich T, Seibel PN, Dandekar T, Müller T. 2008. Unsupervised meta-analysis on diverse gene expression datasets allows insight into gene function and regulation. *Bioinform Biol Insights*. 2:265–280.

Fantini J. 2007. Interaction of proteins with lipid rafts through glycolipid-binding domains: biochemical background and potential therapeutic applications. *Curr Med Chem*. 14:2911–2917.

Gage MJ, Rane SG, Hockerman GH, Smith TJ. 2002. The virally encoded fungal toxin KP4 specifically blocks L-type voltage-gated calcium channels. *Mol Pharmacol*. 61:936–944.

Goldstein IJ, Winter HC, Aurandt J, Confer L, Adamson JT, Hakansson K, Remmer H. 2007. A new α-galactosyl-binding protein from the mushroom *Lyophyllum decastes*. *Arch Biochem Biophys*. 467:268–274.

Grahn E, Askarieh G, Holmner A, Tateno H, Winter HC, Goldstein IJ, Krengel U. 2007. Crystal structure of the *Marasmius oreades* mushroom lectin in complex with a xenotransplantation epitope. *J Mol Biol*. 369:710–721.

Gu F, Khimani A, Rane SG, Flurkey WH, Bozarth RF, Smith TJ. 1995. Structure and function of a virally encoded fungal toxin from *Ustilago maydis*: A fungal and mammalian Ca^{2+} channel inhibitor. *Structure*. 3:805–814.

Guerardel Y, Kol O, Maes E, Lefebvre T, Boilly B, Davril M, Strecker G. 2000. O-glycan variability of egg-jelly mucins from *Xenopus laevis*: Characterization of four phenotypes that differ by the terminal glycosylation of their mucins. *Biochem J*. 352:449–463.

Hendrickson WA. 2013. Evolution of diffraction methods for solving crystal structures. *Acta Crystallogr A*. 69:51–59.

Hendrickson WA, Teeter MM. 1981. Structure of the hydrophobic protein crambin determined directly from the anomalous scattering of Sulfur. *Nature*. 290:107–113.

Iwasa M, Kaito M, Horiike S, Yamamoto M, Sugimoto R, Tanaka H, Fujita N, Kobayashi Y, Adachi Y. 2006. Hepatotoxicity associated with *Lyophyllum decastes* Sing. (Hatakeshimeji). *J Gastroenterol*. 41:606–607.

Johannes L, Römer W. 2010. Shiga toxins – from cell biology to biomedical applications. *Nat Rev Microbiol*. 8:105–116.

Kabsch W. 2010. XDS. *Acta Crystallogr D Biol Crystallogr*. 66:125–132.

Kadirvelraj R, Grant OC, Goldstein IJ, Winter HC, Tateno H, Fadda E, Woods RJ. 2011. Structure and binding analysis of *Polyporus squamosus* lectin in complex with the Neu5Acα2-6Galβ1-4GlcNAc human-type influenza receptor. *Glycobiology*. 21:973–984.

Kashiwagi T, Kunishima N, Suzuki C, Tsuchiya F, Nikkuni S, Arata Y, Morikawa K. 1997. The novel acidophilic structure of the killer toxin from halotolerant yeast demonstrates remarkable folding similarity with a fungal killer toxin. *Structure*. 5:81–94.

Kouki A, Haataja S, Loimaranta V, Pulliainen AT, Nilsson UJ, Finne J. 2011. Identification of a novel streptococcal adhesin P (SadP) protein recognizing galactosyl-α1-4-galactose-containing glycoconjugates: convergent evolution of bacterial pathogens to binding of the same host receptor. *J Biol Chem*. 286:38854–38864.

Krissinel E, Henrick K. 2004. Secondary-structure matching (SSM), a new tool for fast protein structure alignment in three dimensions. *Acta Crystallogr D Biol Crystallogr*. 60:2256–2268.

Krissinel E, Henrick K. 2007. Inference of macromolecular assemblies from crystalline state. *J Mol Biol*. 372:774–797.

Kulkarni KA, Katiyar S, Surolia A, Vijayan M, Suguna K. 2008. Structure and sugar-specificity of basic winged-bean lectin: structures of new disaccharide complexes and a comparative study with other known disaccharide complexes of the lectin. *Acta Crystallogr D Biol Crystallogr*. D64:730–737.

Ling H, Boodhoo A, Hazes B, Cummings MD, Armstrong GD, Brunton JL, Read RJ. 1998. Structure of the shiga-like toxin I B-pentamer complexed with an analogue of its receptor Gb_3. *Biochemistry*. 37:1777–1788.

Liu Q, Dahmane T, Zhang Z, Assur Z, Brasch J, Shapiro L, Mancia F, Hendrickson WA. 2012. Structures from anomalous diffraction of native biological macromolecules. *Science*. 336:1033–1037.

Liu Q, Liu Q, Hendrickson WA. 2013. Robust structural analysis of native biological macromolecules from multi-crystal anomalous diffraction data. *Acta Crystallogr D Biol Crystallogr*. 69:1314–1332.

Lombard V, Golaconda Ramulu H, Drula E, Coutinho PM, Henrissat B. 2014. The carbohydrate-active enzymes database (CAZy) in 2013. *Nucleic Acids Res*. 42:D490–D495.

Mancheño JM, Tateno H, Goldstein IJ, Martínez-Ripoll M, Hermoso JA. 2005. Structural analysis of the *Laetiporus sulphureus* hemolytic pore-forming lectin in complex with sugars. *J Biol Chem*. 280:17251–17259.

McCoy AJ, Grosse-Kunstleve RW, Adams PD, Winn MD, Storoni LC, Read RJ. 2007. Phaser crystallographic software. *J Appl Crystallogr*. 40:658–674.

Miyakawa T, Miyazono K, Sawano Y, Hatano K, Tanokura M. 2009. Crystal structure of ginkbilobin-2 with homology to the extracellular domain of plant cysteine-rich receptor-like kinases. *Proteins*. 77:247–251.

Mølgaard A, Kauppinen S, Larsen S. 2000. Rhamnogalacturonan acetylesterase elucidates the structure and function of a new family of hydrolases. *Structure*. 8:373–383.

Murshudov GN, Skubak P, Lebedev AA, Pannu NS, Steiner RA, Nicholls RA, Winn MD, Long F, Vagin AA. 2011. REFMAC5 for the refinement of macromolecular crystal structures. *Acta Crystallogr D Biol Crystallogr*. 67:355–367.

Pohleven J, Renko M, Magister Š, Smith DF, Künzler M, Štrukelj B, Turk D, Kos J, Sabotič J. 2012. Bivalent carbohydrate binding is required for biological activity of *Clitocybe nebularis* lectin (CNL), the N,N'-diacetyllactosediamine (GalNAcβ1–4GlcNAc, LacdiNAc)-specific lectin from basidiomycete *C. nebularis*. *J Biol Chem*. 287:10602–10612.

Ramagopal UA, Dauter M, Dauter Z. 2003. Phasing on anomalous signal of sulfurs: What is the limit? *Acta Crystallogr D Biol Crystallogr*. 59:1020–1027.

Rao KN, Suresh CG, Katre UV, Gaikwad SM, Khan MI. 2004. Two orthorhombic crystal structures of a galactose-specific lectin from *Artocarpus hirsuta* in complex with methyl-α-D-galactose. *Acta Crystallogr D Biol Crystallogr*. 60:1404–1412.

Sankaranarayanan R, Sekar K, Banerjee R, Sharma V, Surolia A, Vijayan M. 1996. A novel mode of carbohydrate recognition in jacalin, a *Moraceae* plant lectin with a β-prism fold. *Nat Struct Biol*. 3:596–603.

Schubert M, Bleuler-Martinez S, Butschi A, Wälti MA, Egloff P, Stutz K, Yan S, Collot M, Mallet JM, Wilson IBH, et al. 2012. Plasticity of the β-trefoil protein fold in the recognition and control of invertebrate predators and parasites by a fungal defence system. *PLoS Pathog*. 8:e1002706.

Sharma A, Sekar K, Vijayan M. 2009. Structure, dynamics, and interactions of jacalin. Insights from molecular dynamics simulations examined in conjunction with results of X-ray studies. *Proteins*. 77:760–777.

Sheldrick GM. 2008. A short history of SHELX. *Acta Crystallogr A*. 64:112–122.

Shirai T, Watanabe Y, Lee MS, Ogawa T, Muramoto K. 2009. Structure of rhamnose-binding lectin CSL3: Unique pseudo-tetrameric architecture of a pattern recognition protein. *J Mol Biol*. 391:390–403. Erratum in *J Mol Biol*. 412:751.

Strecker G, Wieruszeski JM, Michalski JC, Alonso C, Leroy Y, Boilly B, Montreuil J. 1992. Primary structure of neutral and acidic oligosaccharide-alditols derived from the jelly coat of the Mexican axolotl. Occurrence of oligosaccharides with fucosyl(α1–3)fucosyl(α1–4)-3-deoxy-D-glycero-D-galacto-nonulosonic acid and galactosyl(α1–4)[fucosyl(α1–2)]galactosyl(β1–4)-N-acetylglucosamine sequences. *Eur J Biochem*. 207:995–1002.

Suzuki C, Ando Y, Machida S. 2001. Interaction of SMKT, a killer toxin produced by *Pichia farinosa*, with the yeast cell membranes. *Yeast*. 18:1471–1478.

Suzuki N, Laskowski M Jr, Lee YC. 2004. Phylogenetic expression of Galα1–4Gal on avian glycoproteins: glycan differentiation inscribed in the early history of modern birds. *Proc Natl Acad Sci USA*. 101:9023–9028.

Tempel W, Tschampel S, Woods RJ. 2002. The xenograft antigen bound to *Griffonia simplicifolia* lectin 1-B(4). X-ray crystal structure of the complex and molecular dynamics characterization of the binding site. *J Biol Chem*. 277:6615–6621.

Terwilliger TC. 2000. Maximum-likelihood density modification. *Acta Crystallogr D Biol Crystallogr*. 56:965–972.

Tickle IJ. 2007. Further improvements to AREAIMOL code. *CCP4 Newslett*. 47:20–21.

Ukawa Y, Ito H, Hisamatsu M. 2000. Antitumor effects of (1–>3)-β-D-glucan and (1-–>6)-β-D-glucan purified from newly cultivated mushroom, Hatakeshimeji (*Lyophyllum decastes* Sing.). *J Biosci Bioeng*. 90:98–104.

Vagin A, Teplyakov A. 2010. Molecular replacement with MOLREP. *Acta Crystallogr D Biol Crystallogr*. 66:22–25.

Van Damme EJ, Peumans J, Pusztai A, Bardocz S. 1998. *Handbook of Plant Lectins: Properties and Biomedical Applications*. Wiley: Chichester.

Varrot A, Basheer SM, Imberty A. 2013. Fungal lectins: Structure, function and potential applications. *Curr Opin Struct Biol*. 23:678–685.

Walser PJ, Haebel PW, Künzler M, Sargent D, Kües U, Aebi M, Ban N. 2004. Structure and functional analysis of the fungal galectin CGL2. *Structure*. 12:689–702.

Wälti MA, Walser PJ, Thore S, Grünler A, Bednar M, Künzler M, Aebi M. 2008. Structural basis for chitotetraose coordination by CGL3, a novel galectin-related protein from *Coprinopsis cinerea*. *J Mol Biol*. 379:146–159.

Wimmerova M, Mitchell E, Sanchez JF, Gautier C, Imberty A. 2003. Crystal structure of fungal lectin: six-bladed beta-propeller fold and novel fucose recognition mode for *Aleuria aurantia* lectin. *J Biol Chem*. 278:27059–27067.

Winn MD, Ballard CC, Cowtan KD, Dodson EJ, Emsley P, Evans PR, Keegan RM, Krissinel EB, Leslie AG, McCoy A, et al. 2011. Overview of the CCP4 suite and current developments. *Acta Crystallogr D Biol Crystallogr*. 67:235–242.

Yang N, Li DF, Feng L, Xiang Y, Liu W, Sun H, Wang DC. 2009. Structural basis for the tumor cell apoptosis-inducing activity of an antitumor lectin from the edible mushroom *Agrocybe aegerita*. *J Mol Biol*. 387:694–705.

Yu L, Fernig DG, Smith JA, Milton JD, Rhodes JM. 1993. Reversible inhibition of proliferation of epithelial cell lines by *Agaricus bisporus* (edible mushroom) lectin. *Cancer Res*. 53:4627–4632.

Žurga S, Pohleven J, Renko M, Bleuler-Martinez S, Sosnowski P, Turk D, Künzler M, Kos J, Sabotič J. 2014. A novel beta-trefoil lectin from the parasol mushroom (*Macrolepiota procera*) is nematotoxic. *FEBS J*. 281:3489–3506.